

January 24, 2013

MEMS resonant magnetic field sensor based on an AlN/FeGaB bilayer nano-plate resonator

Yu Hui

Northeastern University

Tianxiang Nan

Northeastern University

Nian Sun

Northeastern University

Matteo Rinaldi

Northeastern University

Recommended Citation

Hui, Yu; Nan, Tianxiang; Sun, Nian; and Rinaldi, Matteo, "MEMS resonant magnetic field sensor based on an AlN/FeGaB bilayer nano-plate resonator" (2013). *Electrical and Computer Engineering Faculty Publications*. Paper 147. <http://hdl.handle.net/2047/d20002863>

MEMS RESONANT MAGNETIC FIELD SENSOR BASED ON AN ALN/FeGaB BILAYER NANO-PLATE RESONATOR

Y. Hui*, T. X. Nan*, N. X. Sun and M. Rinaldi

Department of Electrical and Computer Engineering, Northeastern University,
Boston, Massachusetts, USA

ABSTRACT

This paper reports on the first demonstration of an ultra-miniaturized, high frequency (215 MHz) and high sensitivity MEMS resonant magnetic field sensor based on an AlN/FeGaB bilayer nano-plate resonator capable of detecting magnetic field at nano-Tesla level. Despite of the reduced volume and the high operating frequency of the sensor, high electromechanical performances were achieved (quality factor $Q \approx 511$ and electromechanical coupling coefficient $k_t^2 \approx 1.63\%$). This first prototype was characterized for different magnetic field levels from 0 to 152 Oe showing a frequency sensitivity of ~ 1 Hz/nT and a limit of detection of ~ 10 nT.

INTRODUCTION

The integration of magnetic materials into MEMS technology has achieved much attention in recent years, due to its great advantages in sensing technology [1]. Micromachined resonant magnetic field sensors based on field induced resonance frequency variation of microcantilever resonators with incorporated magnetic materials were previously demonstrated [1,2] but, because of the relatively low electromechanical performance of such resonant devices and their relatively low magnetostrictive coupling, they showed limited values of sensitivity and required the use of complex and off-chip actuation and sensing mechanisms. Moreover, all the previous demonstrations were based on low frequency (\sim KHz) resonant structures; which limits both sensitivity and power handling of the resonant sensor [3].

In this work a stepping stone towards the development of an ultra-miniaturized, power efficient and high resolution magnetic field sensor is set by demonstrating the first prototype of a high frequency (215 MHz) Aluminum Nitride / Iron-Gallium-Boron (AlN/FeGaB) bilayer nano-plate resonant (NPR) magnetic field sensor. Efficient transduction of a high frequency mode of vibration in a strongly magnetostrictive nanoscale resonator is the main challenge associated with the development of high performance MEMS resonant magnetic field sensors. This fundamental challenge is addressed in this work. The efficient on-chip piezoelectric actuation and sensing of a high frequency bulk acoustic mode of vibration in a nano-plate structure, instead of a beam, enables the fabrication of a high frequency and high power handling resonator with power efficient transduction. Low-loss self-biased soft magnetic FeGaB film with a high magnetostriction constant of 70 ppm [4,5] was integrated in the resonant body of an AlN NPR [3] enabling strong magnetomechanical coupling. The strong magnetostrictive coupling between the FeGaB magnetic film and the AlN piezoelectric nano-plate resonator guarantees ultra-high sensitivity of the device resonance frequency to magnetic field. Furthermore, the

electrically conductive magnetostrictive FeGaB thin film is also employed as top floating electrode in the lateral field scheme [3] used to excite vibration in the piezoelectric nano-plate; which enables the achievement of high values of electromechanical coupling coefficient, k_t^2 , comparable to the ones of conventional AlN NPRs [3].

DESIGN AND FABRICATION

The 3-dimensional schematic representation of the proposed MEMS resonant magnetic field sensor is shown in Figure 1. The sensor consists of a bilayer (magnetostrictive layer and piezoelectric layer) nano-plate in which an interdigital transducer (IDT) is employed to excite and sense a higher order contour-extensional mode of vibrations by piezoelectric transduction [3]. The resonance frequency of the device is sensitive to external magnetic field through the equivalent Young's Modulus, E_{eq} , change induced by the external magnetic field (Eq. 1).

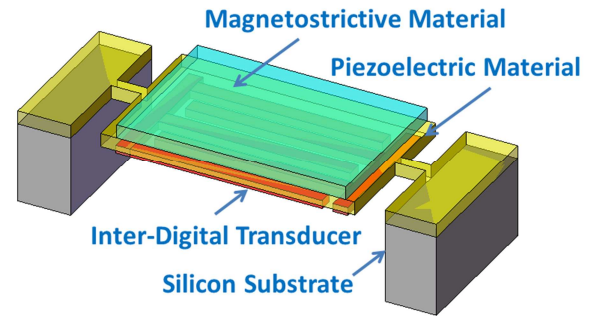


Figure 1: 3D schematic representation of the proposed MEMS resonant magnetic field sensor. It consists of top magnetostrictive material, bottom IDT and piezoelectric material in between.

The resonance frequency of the proposed device is determined by the pitch, W_0 , of the finger electrodes forming the interdigital transducer (IDT) (Figure 2 (a)), and the material properties: equivalent Young's Modulus E_{eq} and density ρ_{eq} , by (1) [6]. When the sensor is exposed to an external magnetic field, the equivalent Young's Modulus of the overall structure is changed due to the magnetostrictive effect [4] of the magnetic material, resulting in a shift of the device resonance frequency.

$$f = \frac{1}{2W_0} \sqrt{\frac{E_{eq}}{\rho_{eq}}} \quad (1)$$

The bilayer nano-plate-resonant magnetic field sensor proposed in this work was implemented using FeGaB as magnetic layer and AlN as piezoelectric layer (Figure 1). The fabricated device is shown in Figure 2. The effective device sensing area was designed to be $100 \mu\text{m} (W) \times 200$

μm (L), and the pitch, W_0 , of bottom Platinum (Pt) finger-electrode was set to be $11\ \mu\text{m}$ (Figure 2 (a)), resulting in a high order contour-extensional mode [3] resonator working at high resonance frequency of 215 MHz. The thicknesses of the AlN piezoelectric layer and the FeGaB magnetostrictive layer were set to be the same (250 nm) in order to achieve high magnetostrictive coupling between the magnetic and piezoelectric layers.

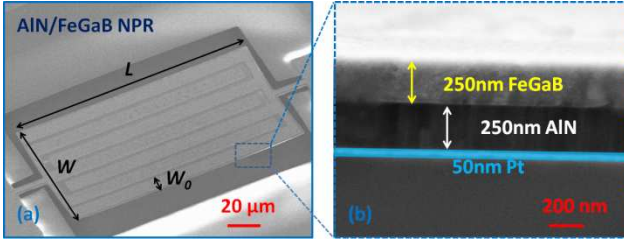


Figure 2: (a) SEM image of the fabricated MEMS resonant magnetic field sensor; (b) SEM cross-section of the material stack forming the resonant magnetic field sensor.

The AlN/FeGaB NPR magnetic field sensor of this work was fabricated using a five-mask microfabrication process, shown in Figure 3. A high resistivity Silicon (Si) wafer ($>10000\ \Omega\cdot\text{cm}$) was used as substrate. A 50 nm thick Platinum (Pt) film was sputter-deposited and patterned by lift-off on top of the Si substrate to define the bottom IDT. Then, the 250 nm AlN film (stress 60 MPa and FWHM 2.2°) was sputter-deposited and vias to access the bottom IDT electrode were etched by H_3PO_4 . Next, the 250 nm thick FeGaB magnetic layer was deposited by Physical Vapor Deposition (PVD) and patterned by lift-off. A 100 Oe in-situ magnetic field bias was applied during the PVD deposition along the width, W , of the device (Figure 2) to pre-orient the magnetic domains. Then, a 50 nm thick gold (Au) film was evaporated and patterned by lift-off to form the top electrode. After that, the AlN film was etched by Inductively Coupled Plasma (ICP) etching in Cl_2 based chemistry to define the shape of the resonant nano-plate. Finally, the structure was released by XeF_2 isotropic etching of the Silicon substrate.

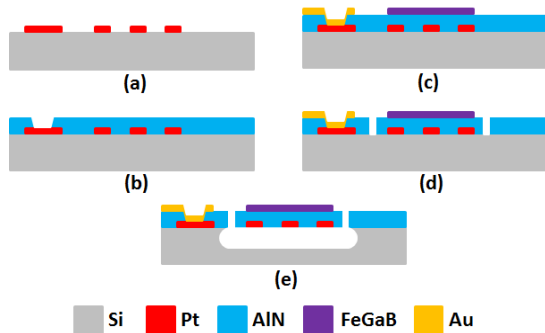


Figure 3: Microfabrication processes: (a) sputter deposition and lift off of the Pt bottom electrode; (b) sputter deposition of AlN and wet etch in H_3PO_4 to open vias; (c) sputter deposition and lift off of the FeGaB magnetic layer and the Au top probing pads; (d) dry (ICP) etching of the AlN film in Cl_2 based chemistry; (e) dry release of the resonator by XeF_2 isotropic etching.

EXPERIMENTAL RESULTS

The fabricated MEMS resonant magnetic field sensor was tested using the measurement setup illustrated in Figure 4. The sensor was tested in a RF probe station and a DC magnetic field from 0 to 152 Oe was applied by a Helmholtz coil to the sensor along the length, L , of the device.

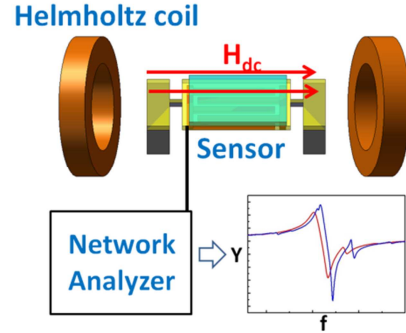


Figure 4: Schematic illustration of the measurement setup: DC magnetic field (0-152 Oe) is applied to the magnetic field sensor by a Helmholtz coil and the change of the device admittance is monitored by a network analyzer.

The electrical response of the fabricated AlN/FeGaB nano-plate resonator was tested by an Agilent 8350b network analyzer after performing a short-open-load calibration on a reference substrate. The measured admittance and Butterworth-Van Dyke (BVD) fitting curves versus frequency are shown in Figure 5. The resonance frequency of the device was measured to be 215 MHz and the quality factor Q and electromechanical coupling coefficient k_t^2 were extracted to be 511 and 1.63%. Such high k_t^2 was achieved due to the electrically conductive magnetostrictive FeGaB film as top floating electrode in the lateral field scheme [3], which offers better confinement of the electric field within the entire thickness of the AlN film [7], used to excite lateral vibration through d_{31} piezoelectric coefficient in the piezoelectric nano-plate. Despite the device volume reduction, the high frequency operation and the loading effect of the FeGaB layer, a high quality factor of 511 is achieved. Optimization of AlN and FeGaB layer thicknesses for maximum $k_t^2 \cdot Q$ will be investigated in future.

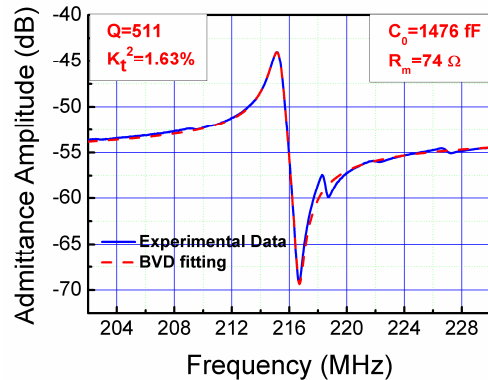


Figure 5: Measured admittance and BVD model fitting of the fabricated 215 MHz AlN/FeGaB NPR magnetic field

sensor. C_0 is the device equivalent geometrical capacitance and R_m is the motional resistance.

To test the response of the device, four different levels of DC magnetic field ranging from 0 to 152 Oe were applied to the sensor by the Helmholtz coil. Figure 6 shows the measured admittance corresponding to these four levels of magnetic field. The measurement clearly indicates that the admittance amplitude, the quality factor and the resonance frequency of the device were modulated by the externally applied magnetic field. Therefore, DC magnetic field can be detected by tracking any of these three parameters. Resonance frequency and admittance amplitude sensitivities were both exploited in this work, resulting in a high sensitivity (~ 1 Hz/nT) and low limit of detection (~ 10 nT) MEMS resonant magnetic field sensor.

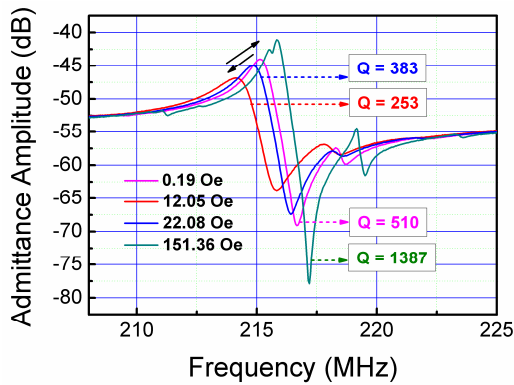


Figure 6: Measured admittance curves and extracted mechanical quality factor, Q , of the AlN/FeGaB NPR magnetic field sensor under different DC magnetic field levels varying from 0.19 Oe to 151.36 Oe. The variation in Q is attributed to a change in acoustic loss due to reorientation of the magnetic domains under external magnetic field.

The fabricated MEMS resonant magnetic field sensor was calibrated for DC magnetic field from 0 to 152 Oe by monitoring the resonance frequency and admittance amplitude (at the resonance frequency). The measured resonance frequency shift and admittance amplitude change are shown in Figure 7. Both the resonance frequency and the admittance amplitude of the device decrease at first when a small magnetic field bias is applied (0-10 Oe) and increase when a relatively larger magnetic field bias (10-50 Oe) is applied. Finally, by further increasing the magnetic field (> 50 Oe), the device response saturates.

The frequency shift of the resonant sensor is attributed to the Young's Modulus variation (ΔE effect) [2] of the AlN/FeGaB resonant structure under DC biased magnetic field. As the FeGaB magnetic film was deposited with 100 Oe in-situ magnetic field bias applied along the width, W , of the device (Figure 2 (a)), a pre-orientation of magnetic domains was caused. When the magnetic field to be detected is applied along the length, L , of the device, a reorientation of the magnetic domains is induced which causes a decrease of the Young's Modulus to its minimum when the applied magnetic field

cancels its intrinsic anisotropy field. By further increasing the amplitude of the magnetic field, the Young's Modulus increases and reaches its maximum at the saturation of magnetization, with no reorientation of magnetic domains.

As for the admittance amplitude, it is mainly determined by the motional resistance, R_m , at the resonance. The values of R_m can be extracted by the equivalent BVD model fitting which shows that R_m increases first with increasing magnetic field and reaches its maximum at around 10 Oe, then it decreases when the amplitude of the applied magnetic field is further increased. The change of R_m could be attributed to the Young's Modulus and acoustic loss variations due to reorientation of the magnetic domains under external magnetic field. Since the admittance amplitude is inversely proportional to R_m , it shows an opposite trends of R_m changing, but the same trends of resonance frequency shift, shown in Figure 7. Figure 7 indicates that a high sensitivity magnetic sensor can be implemented by exploiting the region 0 – 10 Oe or 10 – 50 Oe of the sensitivity curve. For small magnetic field sensing (0 – 10 Oe), the measured resonance frequency sensitivity to DC magnetic field is approximately 1 Hz/nT.

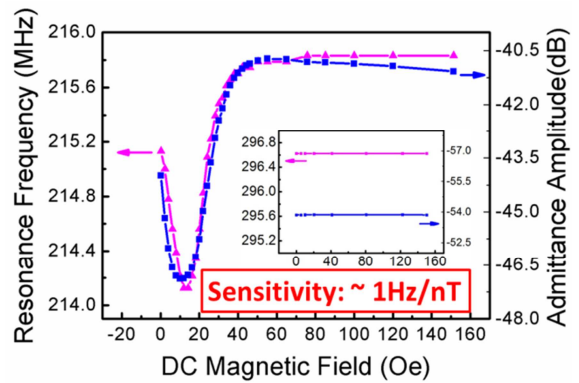


Figure 7: Measured resonance frequency and admittance amplitude (at the resonance frequency) of the device for different values of DC magnetic field applied along the length, L , of the resonator. The inset shows the response of a reference AlN NPR without magnetic material. As expected, the resonance frequency of the reference device does not change.

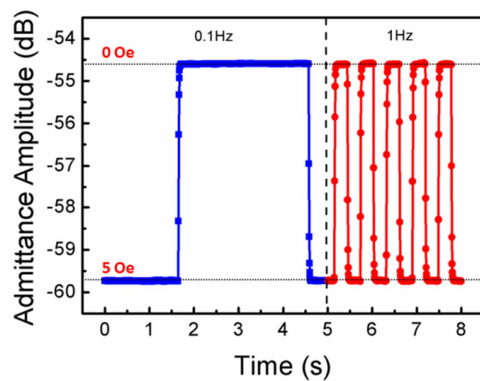


Figure 8: Time domain measurement of the device admittance amplitude (close to resonance frequency) in response to low frequency (0.1 Hz, 1 Hz) square wave magnetic field.

The transient response of the device was measured by exciting the sensor at a single frequency, f_c , and monitoring the variation over time of the device admittance amplitude [8]. The excitation frequency, $f_c = 215.9$ MHz, was set between the series and parallel resonances, where the slope of admittance amplitude curve versus frequency is maximum [8]. The measured transient response of the sensor under low frequency (0.1 Hz and 1 Hz) square wave magnetic field applied is shown in Figure 8.

In order to explore the limit of detection of the fabricated MEMS resonant magnetic field sensor, extremely low levels of magnetic field (from 4 nT to 100 nT) were applied to the sensor and the corresponding admittance amplitude change was monitored (Figure 9). The measurement result shows that DC magnetic field as low as 10 nT can be detected by monitoring the admittance amplitude (admittance amplitude change of 0.004 dB versus noise level of ~ 0.004 dB), indicating the great potential of this prototype to be used for detecting extremely low levels of magnetic field.

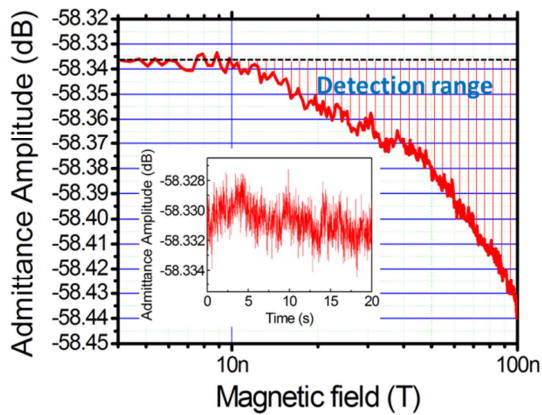


Figure 9: Admittance amplitude response under extremely small magnetic field bias applied to the sensor. Magnetic field as low as 10 nT can be detected by monitoring the admittance amplitude change. The inset shows the noise level of the admittance amplitude is 0.004 dB.

CONCLUSION

In this paper, an ultra-miniaturized, high frequency and high sensitivity MEMS resonant magnetic field sensor based on an AlN/FeGaB bilayer nano-plate resonator capable of detecting magnetic field at nano-Tesla level was designed, fabricated and tested. For the first time a highly magnetostrictive and magnetically soft FeGaB thin film (250 nm thick) was integrated in the resonant body of a high frequency AlN resonant nano-plate (250 nm thick) resulting in an innovative MEMS resonant structure whose resonance frequency is highly sensitive to external magnetic field. Despite the reduced volume and the high operating frequency of such AlN/FeGaB NPR, high electromechanical performances were achieved (quality factor $Q \approx 511$ and electromechanical coupling coefficient $k_t^2 \approx 1.63\%$) enabling the demonstration of an ultra-miniaturized and high resolution magnetic field sensor. This first prototype was characterized for different magnetic field levels ranging from 0 to 152 Oe showing a frequency sensitivity

of ~ 1 Hz/nT and an experimental limit of detection of 10 nT, indicating the great potential of this prototype for detecting extremely low levels of magnetic field.

ACKNOWLEDGEMENTS

The authors wish to thank the staff of the George J. Kostas Nanoscale Technology and Manufacturing Research Center at Northeastern University and Dr. Songbin Gong at the University of Pennsylvania for the help with the XeF₂ etching process.

REFERENCES

- [1] T. C. Leichle, M. von Arx and M. G. Allen, "A micromachined resonant magnetic field sensor", *IEEE MEMS 2001 Conference*, Interlaken, Jan 21-25, 2001, pp. 274-277.
- [2] B. Gojdka, R. Jahns, K. Meurisch, H. Greve, R. Adelung, E. Quandt, R. Knochel and F. Faupel, "Fully integrable magnetic field sensor based on delta-E effect", *Appl. Phys. Lett.*, vol. 99, 2011, pp. 223502.
- [3] M. Rinaldi and G. Piazza, "Effects of volume and frequency scaling in AlN contour mode NEMS resonators on oscillator phase noise" *IEEE IFCS 2011 Conference*, San Francisco, May 1-5, 2011, pp. 1-5.
- [4] J. Lou, M. Liu, D. Reed, Y. H. Ren and N. X. Sun, "Giant electric field tuning of magnetism in novel multiferroic FeGaB/Lead Zinc Niobate Lead Titanate heterostructures" *Advanced Materials*, vol. 21, 2009, pp. 4711-4715.
- [5] J. Lou, R. E. Insignares, Z. Cai, K. S. Ziemer, M. Liu and N. X. Sun, "Soft magnetism, magnetostriction, and microwave properties of FeGaB thin films", *Appl. Phys. Lett.*, vol. 91, 2007, pp. 182504.
- [6] M. Rinaldi C. Zuniga and G. Piazza, "5-10 GHz AlN contour-mode nanoelectromechanical resonators" *IEEE MEMS 2009 Conference*, Sorrento, Jan 24-28, 2009, pp. 916-919.
- [7] G. Piazza, P. J. Stephanou and A. P. Pisano, "One and two port piezoelectric higher order contour-mode MEMS resonators for mechanical signal processing", *Solid-State Electronics*, vol. 51, 2007, pp. 1596-1608.
- [8] M. Rinaldi, C. Zuniga and G. Piazza, "Ultra-thin-film AlN contour-mode resonators for sensing applications", *IEEE IUS 2009 Conference*, Rome, Sept 20-23, 2009, pp. 714-717.

CONTACT

*Y. Hui, tel: +1-617-7589518; hui.y@husky.neu.edu

* These authors contributed equally to this work.